JOURNAL OF GEOPHYSICAL RESEARCH, VOL. 105, NO. D6, PAGES 7089–7101, MARCH 27, 2000

Temperature dependence of the absorption cross sections of formaldehyde between 223 and 323 K in the wavelength range 225–375 nm

Richard Meller and Geert K. Moortgat

Atmospheric Chemistry Department, Max-Planck-Institut für Chemie, Mainz, Germany

Abstract. UV absorption cross sections of formaldehyde (HCHO) have been measured with a spectral resolution of 0.025 nm in the wavelength range 225–375 nm at 298 K using a diode array detector. At selected temperatures ranging from 223 to 323 K, measurements have been conducted to obtain temperature gradients in the wavelength range 250–356 nm. Error limits for the reported absorption cross sections are ±5% but at least $\pm 3 \times 10^{-22}$ cm^2 molecule^{-1}. For the temperature gradients, uncertainties are <8%. Spectra and temperature gradients are compared with earlier measurements.

1. Introduction

Formaldehyde is the most important and most abundant organic carbonyl compound in the atmosphere. It has been observed in both the polluted urban and rural troposphere. Typical formaldehyde concentrations in urban areas are of the order of 2–16 ppbv [*Grosjean*, 1991; *Grosjean et al.*, 1993], in the rural areas are between 1 and 4 ppbv [*Benning and Wahner*, 1998; *Fried et al.*, 1997; *Harder et al.*, 1997; *Lee et al.*, 1995, 1998], in clean remote air are between 0.1 and 0.5 ppbv [*Heikes et al.*, 1996; *Lowe and Schmidt*, 1983], and in the upper troposphere are <0.1 pptv [*Jacob et al.*, 1996]. Formaldehyde is a primary emission product from fossil fuel combustion [*Anderson et al.*, 1996; *Altshuller*, 1993; *Carlier et al.*, 1986] and from biomass burning [*Carlier et al.*, 1986; *Lipari et al.*, 1984]. It is also formed in the atmosphere as a secondary product in the photochemical oxidation of methane and higher hydrocarbons [*Altshuller*, 1993; *Carlier et al.*, 1986; *Levi*, 1971] and in the ozonolysis of 1-alkenes [*Atkinson et al.*, 1995; *Grosjean et al.*, 1996]. The main removal processes in the troposphere during daylight are reaction with OH radicals and photolysis. Removal by wet and dry deposition can be important during the night [*Altshuller*, 1993; *Lowe and Schmidt*, 1983].

The absorption of solar radiation of formaldehyde results in the photodissociation by the following primary processes (1) and (2) [*Moortgat et al.*, 1980, 1983].

(R1) $\mathrm{HCHO} + h\nu\,(\lambda < 340\ \mathrm{nm}) \rightarrow \mathrm{HCO} + \mathrm{H}$

(R2) $\mathrm{HCHO} + h\nu\,(\lambda < 365\ \mathrm{nm}) \rightarrow \mathrm{CO} + \mathrm{H_2}$

Reaction (R1) forms formyl radicals and hydrogen atoms (source for HO_2 from secondary reactions), whereas (R2) forms carbon monoxide and molecular hydrogen. Both reaction pathways ultimately yield a CO molecule, but in the radical channel (R1), there are also two hydroperoxy radicals formed (via (R3) and (R4)), which contribute to the odd hydrogen budget.

(R3) $\mathrm{HCO} + \mathrm{O_2} \rightarrow \mathrm{HO_2} + \mathrm{CO}$

Paper number 1999JD901074.
0148-0227/00/1999JD901074$09.00

(R4) $\mathrm{H} + \mathrm{O_2} + \mathrm{M} \rightarrow \mathrm{HO_2} + \mathrm{M}$

The chemistry of formaldehyde plays an important role in the radical chemistry of the troposphere, especially in the upper troposphere. One important in situ source of formaldehyde is the photolysis of acetone, which yields two HCHO molecules under conditions where $[\mathrm{NO}] \gg [\mathrm{HO_2}]$ [*Singh et al.*, 1995]. However, as *Jaegle et al.* [1998] showed, direct convective injection of peroxides and formaldehyde from the boundary layer into the upper troposphere is also expected to resolve the discrepancies between observed and modeled OH and HO_2 concentrations. In order to model the HO_x chemistry of the upper troposphere and lower stratosphere correctly and to calculate the atmospheric lifetime of formaldehyde it is very important to know precisely the rate constant of the reaction HCHO + OH and the photolysis rate of formaldehyde.

Another important application where accurate absolute absorption cross sections are needed is in satellite-based remote sensing of atmospheric trace gases and pollutants. For example, *Thomas et al.* [1998] reported column distributions of HCHO and NO_2 in severe rain forest biomass burning events over southeast Asia measured by the Global Ozone Monitoring Experiment (GOME) using differential optical absorption spectroscopy (DOAS). In this technique, reference spectra of trace gases with unique absorption features are used in a multilinear regression to match optical densities in the backscattered light from the Earth's atmosphere. For both applications, modeling and remote sensing, it is crucial to know the exact absorption cross sections and their temperature dependence.

Interest in the spectroscopy of formaldehyde has existed for almost a century and has played a key role in many aspects of the understanding of polyatomic molecules. The highly structured absorption features have been subject of many studies ever since the first detailed investigations of *Henri and Schou* [1928] in 1928. *Dieke and Kristiakowsky* [1934] were the first to accomplish a conclusive rotational analysis for a number of absorptions bands in a classical investigation, which resulted in the first unambiguous interpretation of an electronic spectrum of a polyatomic molecule.

The first measurements of the absorption cross section of formaldehyde in the UV/visible region were published by *McQuigg and Calvert* [1969] in 1969 (integrated absorption cross sections from their work are given by *Calvert et al.* [1972]). A

decade later in 1980, *Bass et al.* [1980] and *Moortgat et al.* [1980] and, more recently, in 1990, *Cantrell et al.* [1990] and *Rogers* [1990] reported measurements that reflect improvements in the instrumental techniques and in the computational possibilities in calculating photodissociation coefficients. *McQuigg and Calvert* [1969], *Bass et al.* [1980], and *Moortgat et al.* [1980] used conventional scanning spectrometers, whereas *Cantrell et al.* [1990] and *Rogers* [1990] applied Fourier transform spectroscopy. An overview of all the previous measurements, techniques, and the experimental details is presented in Table 1 and should be consulted for further details such as resolution or temperature. Even though the existence of the temperature dependence of the absorption cross sections of formaldehyde has been known for a long time, only the studies of *Bass et al.* [1980] and *Cantrell et al.* [1990] reported measurements at different temperatures and considered the temperature effects on the atmospheric lifetime of formaldehyde.

The evaluations from the International Union of Pure and Applied Chemistry (IUPAC) Subcommittee on Gas Kinetic Data Evaluation for Atmospheric Chemistry [*Atkinson et al.*, 1997] and the NASA Panel for Data Evaluation [*DeMore et al.*, 1997] (see introduction sections of both evaluations for references of older issues) recommended in their 1980 and 1981 publications, respectively, the available data from *Calvert et al.* [1972]. From 1983 to 1990 the NASA panel recommended an average of the spectra from *Bass et al.* [1980] and *Moortgat et al.* [1980] on the basis of the IUPAC recommendation from 1982. Since 1992 the IUPAC has recommended the use of G. K. Moortgat and W. Schneider data (unpublished, 1985) at 285 K for λ = 240–300 nm and the temperature-dependent *Cantrell et al.* [1990] data for λ = 300–357.5 nm, whereas the NASA panel only gave the temperature-dependent *Cantrell et al.* [1990] data for wavelengths larger than 300 nm. The spectrum of *Rogers* [1990] was not considered in these evaluations, although it is in good agreement with the *Cantrell et al.* [1990] spectrum. In the IUPAC report from 1992 the failure of *Rogers* [1990] to observe nonlinearity in the absorbance of HCHO as a function of the HCHO concentration was the reason given for discharging his work.

Despite the importance of the photolysis of HCHO for atmospheric chemistry, there is no study that satisfies all requirements of an absorption spectrum for the use in laboratory work and model calculations. The spectra of *Calvert et al.* [1972] and *Moortgat et al.* [1980] reveal a lack of resolution; the published data by *Cantrell et al.* [1990] only cover a limited range of the whole spectrum; *Bass et al.* [1980] and *Rogers* [1990] have obvious problems with strong absorption bands between 320 and 350 nm and at wavelengths shorter than 280 nm, respectively. Resulting from these problems, the temperature gradient is also fairly uncertain. These insufficiencies made new measurements at atmospheric temperatures necessary.

2. Experimental Methods

2.1. Apparatus

Absorption measurements were carried out in a spectrophotometric apparatus equipped with a diode array detector as described in detail by *Meller et al.* [1991] and *Meller and Moortgat* [1997]. Only main features are described in short. The 63 cm (optical path) cell with an inner diameter of 30 mm was provided with two suprasil windows at both sides forming an evacuated compartment to prevent condensation of water vapor. The cell was connected to a standard greaseless vacuum system, and pressure measurements were made with Baratron gauges (MKS). The accuracy of the manometer is specified to be better than 0.15% in the pressure range used. The temperature of the cell could be regulated in the range 220–350 K by circulating a cooling liquid through the jacket of the cell. Temperatures were measured by means of a PT100 sensor connected directly to the cell. The absolute uncertainties were ~1 K at low temperatures, and the stability during the measurements was ±0.1 K. Depending on the wavelength range measured, one of two power and temperature stabilized light sources was employed. A 200 W deuterium lamp (Heraeus) was used for the wavelength region 220–310 nm, and a 60 W commercial tungsten/halogen lamp was used for wavelengths above 300 nm. The light passed a filter before entering the cell. A UG5 filter in the region above 250 nm and a BG24 filter below 250 nm were used to prevent stray light. The light was dispersed by a 60 cm Czerny-Turner-type monochromator equipped with a holographic grating with 3600 grooves mm^{-1}, yielding a spectral resolution of 0.025 nm. The transmitted light was detected by a 25 mm 1024 pixel silicon diode array detector (EG&G models 1412 and 1461). An entrance slit of the monochromator was set to 25 μm for optimal resolution of the diode array.

Wavelength calibration of the detector was performed in air at ~750 Torr using the emission lines of either a Zn/Cu, Ir/Ni, or Fe hollow cathode lamp (Cathodeon, Cambridge). For each spectral window, about ten emission lines given by *Crosswhite* [1975] or by *Massachusetts Institute of Technology (MIT)* [1969] were used to calculate a quadratic calibration ($\lambda = a + bn + cn^2$, where n is the number of diodes) to yield a wavelength calibration with an accuracy of better than 0.003 nm. The determination of the spectral resolution was based on measurements of the half width of several emission lines of the used hollow cathode lamps. The resolution in a single measurement varied between 0.028 at 230 nm and 0.021 at 360 nm. However, in the final spectrum for the entire wavelength range the resolution is somewhat lower (~0.04 nm) because of the later data handling and manipulation to account for the nonlinearity in the projection of the dispersed light on the diode array and to match the wavelength calibration of the data sets obtained in different spectral resolutions.

A single measurement by the diode array spectrometer encompassed typically a wavelength range of 7 nm, representing a spectral window for a specific wavelength range. The exposure time (on-chip integration time) of the array detector varied between 5 and 120 s. About six measurements were made for each spectral window, and each adjacent window overlapped at least half of the previous and the following ones. For the spectral range of λ = 225 − 375 nm, more than 300 single measurements were made and are combined in the final spectrum. All measurements for the final spectrum were made at 500 ± 50 mtorr (1 torr = 133 Pa) HCHO partial pressure except the region below 265 nm. In this region, pressures up to 5 Torr were used. No bath gas was used in the measurements presented here. Formaldehyde tends to polymerize and to absorb onto the walls during the handling and the measurements. To avoid these problems it was necessary to fill the cell rapidly, to use very low HCHO partial pressures and to have short residence times in the cell.

Uncertainties in the measured optical path length, temperature, pressure, sample purity, and absorbance contribute to the overall uncertainty in the measured absorption cross sec-

Table 1. Summary of Measurements of Absorption Cross Sections of Formaldehyde

Source	HCHO Generation	Instrument	Cell Path Length	Measured Resolution	Reported Resolution	Temperature	Wavelength Range, nm	HCHO Pressure	Total Pressure torr/bath gas
McQuigg and Calvert [1969]	from the polymer by a procedure after *Spence and Wild* [1935], stored at −78°C before use	low-resolution recording spectrometer (Bausch and Lomb 505)	water-jacketed cell, 5 cm	n.a.	10 nm	353 K	285–365	n.a.	n.a.
Bass et al. [1980]	heated a mixture of paraformaldehyde and P_2O_5 to 100°C, purified by vacuum distillation, and stored in the dark at 77 K before used	hydrogen light source, 0.75m Ebert grating-monochromator, beam splitter, absorption cell, PMTs	temperature-controlled cell variable path length through multiple reflection mirrors	0.05 nm	atmospheric intervals, and 10 nm*	296 and 223 K	260–365	0.5–5.0 torr	100/He
Moortgat et al. [1980]	heated paraformaldehyde to 150°C, trapped vapor by dry ice, performed trap to trap distillation, stored in the dark at 77 K	double beam spectrometer, D_2 lamp, Czerny-Turner-type scanning monochromator	fused quartz cell, optical path length 8.0 cm	0.5 nm	plot	thirteen different temperatures between 210 and 363 K	230–365	5–20 torr	/none
Cantrell et al. [1990]	heated paraformaldehyde to 360 K, trapped monomer at 77 K, degassed, and stored before use	Bomem DA 3.01 FT spectrometer, high pressure stabilized xenon arc lamp, aluminum-coated quartz beamsplitter, wideband PMT	temperature-controlled, stainless steel cell, 20.0 cm optical path	1.00 cm^{-1} (~0.001 at 310 nm)	atmospheric intervals and individual band intensities*	eight different temperatures between 223 and 293 K	300–360	6 different pressures (10 torr)	500/N_2
Rogers [1990]	heated paraformaldehyde, condensed monomer in liquid N_2 trap, purified by trap to trap distillation	Bomem DA 3.15 FT spectrometer with a deuterium UV lamp and a silicon/UV detector	4.6 cm diameter Pyrex gas cell, 99 cm long	0.01–0.04 nm	10 nm*	296 ± 2 K	235–365	0.8–9 torr	0–760/air
This work	heated paraformaldehyde, passed through ethanol-dry ice trap, used immediately	D_2 or tungsten/halogen lamp, 60 cm monochromator, halographic grating, diode array detector	Temperature controlled 63-cm cell	0.021–0.028 nm	1 nm and atmospheric intervals*	225–375 K, four different temperatures	225–375	0.5–5 torr	/none

PMT, photomultiplier tube; n.a., not available.
*High-resolution spectra (in the measured resolution) were also available

tions. The path length could be measured to better than 3 mm, which corresponds to a maximum error of 0.5%. At ambient temperatures the accuracy of the temperature measurement was ~0.1%, but at lower temperatures, it increased to almost 1%. The quoted uncertainties in the pressure measurements were <0.15%. As stated in section 2.2, the purity of the sample was expected to be better than 99.5%. The baseline fluctuations were <0.1% as determined by measuring $I_o(\lambda)$ after pumping out and before filling the absorption cell. The precision of the absorbance measurements was ±3% RMS. We estimate the absolute uncertainty to be ±5% RMS for absorption cross sections larger than 5×10^{-21} cm^2 molecule^{-1} but to be at least $\pm 3 \times 10^{-22}$ cm^2 molecule^{-1}.

2.2. HCHO Generation

HCHO was obtained from paraformaldehyde by a procedure patterned after that of *Spence and Wild* [1935]. The monomeric gas-phase formaldehyde was prepared by gently heating the paraformaldehyde (Merck) in a glass tube, which was connected to the vacuum system. The gas passed a wad of glass wool to hold back particles and an ethanol-dry ice trap to remove the water. Then the gas was filled directly into the absorption cell. The purity of the product was checked by Fourier transform infrared (FTIR) spectroscopy. No signs of water, carbon monoxide, or carbon dioxide could be detected. The purity was better than 99.5%. This value was obtained by summing up the detection limit of the contaminants. Experiments with HCHO trapped and stored at 77 K gave lower and nonreproducible results (see section 3). Only fresh prepared HCHO was used for the measurements.

3. Results and Discussion

3.1. Absorption Cross Sections at 298 K

Before measuring the HCHO absorption cross sections, experiments were performed to investigate the effect of the HCHO partial pressure, of the total pressure, and of different methods of storing HCHO on the absorption spectra. These tests were performed to determine the best experimental conditions for the measurements.

UV absorption spectra were recorded for pure HCHO with pressures ranging from 0.5 to 5 torr, and no buffer gas added. Strong deviations from the Beer-Lambert law were observed for the strong absorption lines with cross sections larger than 4×10^{-20} cm^2 molecule^{-1}. Absorption cross sections at the peaks of vibrational bands were decreasing by ~25% over the pressure range from 0.5 to 5 torr. For cross sections smaller than 1×10^{-20} cm^2 molecule^{-1}, no or only slight deviations from the Beer-Lambert law were observed. For this study only spectra with HCHO partial pressures of 500 ± 50 mtorr were used to calculate the absorption cross sections in the wavelength range from 265 to 355 nm. At this pressure the measured cross sections for the strong absorptions are only ~2% lower than the values one would obtain from the extrapolation to zero pressure.

Experiments were also performed in which the total pressure was varied in the range from 1 to 760 torr to investigate the effects of foreign gas broadening on the HCHO absorption spectrum. Nitrogen (purity 99.999%) was added as a buffer gas. In these measurements for increasing total pressures, decreasing absorption cross sections were observed. The decrease at all wavelengths was of the order of ~25% for the pressure change from 0 to 300 torr N_2. For a further increase to up to 760 torr, no further change was noticed. These observations are in contrast to those of *Cantrell et al.* [1990] where an increase of up to 50% in the absorptions cross sections with increasing foreign gas pressure (up to 800 torr N_2) was detected and to those of *Bass et al.* [1980] where no pressure effect (in 0–600 torr He) was observed. *Cantrell et al.* [1990], who measured at a resolution of ~0.01 nm, explained their observations as a purely instrumental artefact, as the effect of pressure-induced line broadening in conjunction with unresolved spectral features. *Rogers* [1990], who measured with the same resolution as *Cantrell et al.* [1990], reported a foreign gas dependency only for HCHO partial pressures lager than 2 torr, whereas *Moortgat et al.* [1980] noticed minor changes of up to 10% and only for the strong absorption bands. For the study of the total pressure effect, monomeric HCHO was generated as described above and introduced into the absorption cell and then N_2 was added to the desired total pressure. We believe that our observations are only caused by incomplete mixing of the HCHO and N_2 in the absorption cell. The use of evacuated suprasil window inserts in the absorption cell, each reaching 9 cm into the cell, caused "dead volumes" outside of the detection zone, where HCHO was pushed into by the N_2, which was introduced from the middle of the cell. More evidence for this explanation is the fact that the same relative decrease was noticed in the absorption at all wavelengths for each total pressure.

In another set of experiments, monomeric HCHO was generated as described before and stored at 77 K until it was allowed to warm up to room temperature and introduced into the absorption cell. Using this method of sample preparation, the recorded absorption spectra were always lower and less reproducible than these using the "in situ" generation of HCHO, possibly because of reactions of HCHO during sample preparation and storage. Similar experiences were made diluting monomeric HCHO in a 5 L glass bulb with N_2 before using it for absorption measurements in the cell. For these reasons we preferred the in situ generation of HCHO to the procedures where HCHO was stored at lower temperatures.

Absorption cross sections were calculated through the relationship

$$\sigma(\lambda) = \frac{\ln [I_o(\lambda)/I(\lambda)]}{l c_{\mathrm{HCHO}}} \quad (1)$$

where $\sigma(\lambda)$ is the absorption cross section in units of cm^2 molecule^{-1}, I_o and I are the spectral intensities at the wavelength λ at empty and filled cell, respectively, l is the optical pathlength in cm, and c_{HCHO} is the concentration of HCHO in units of molecule cm^{-3}.

In Figure 1 the UV spectrum of HCHO in the wavelength range 225–375 nm at 298 K in an optical resolution of 0.04 nm is shown, and in Table 2, absorption cross sections of HCHO at 298 K averaged over 1 nm intervals are listed. At this point it should be mentioned that the spectrometer for this study was not evacuated and that the wavelengths reported in this work were measured in 750 ± 10 torr air. The air wavelength scale is blue shifted by ~0.07 nm near 230 nm and ~0.10 nm near 360 nm compared to the vacuum wavelengths. In the studies of *Cantrell et al.* [1990] and *Rogers* [1990], vacuum wavelengths were reported, even though it was not stated in the work of *Rogers* [1990]. For comparing these measurements with ours the vacuum wavelengths were transformed into air wavelengths ($\lambda_{\mathrm{air}} = \lambda_{\mathrm{vac}}/n$) using equations (2) and (3) by *Edlen*

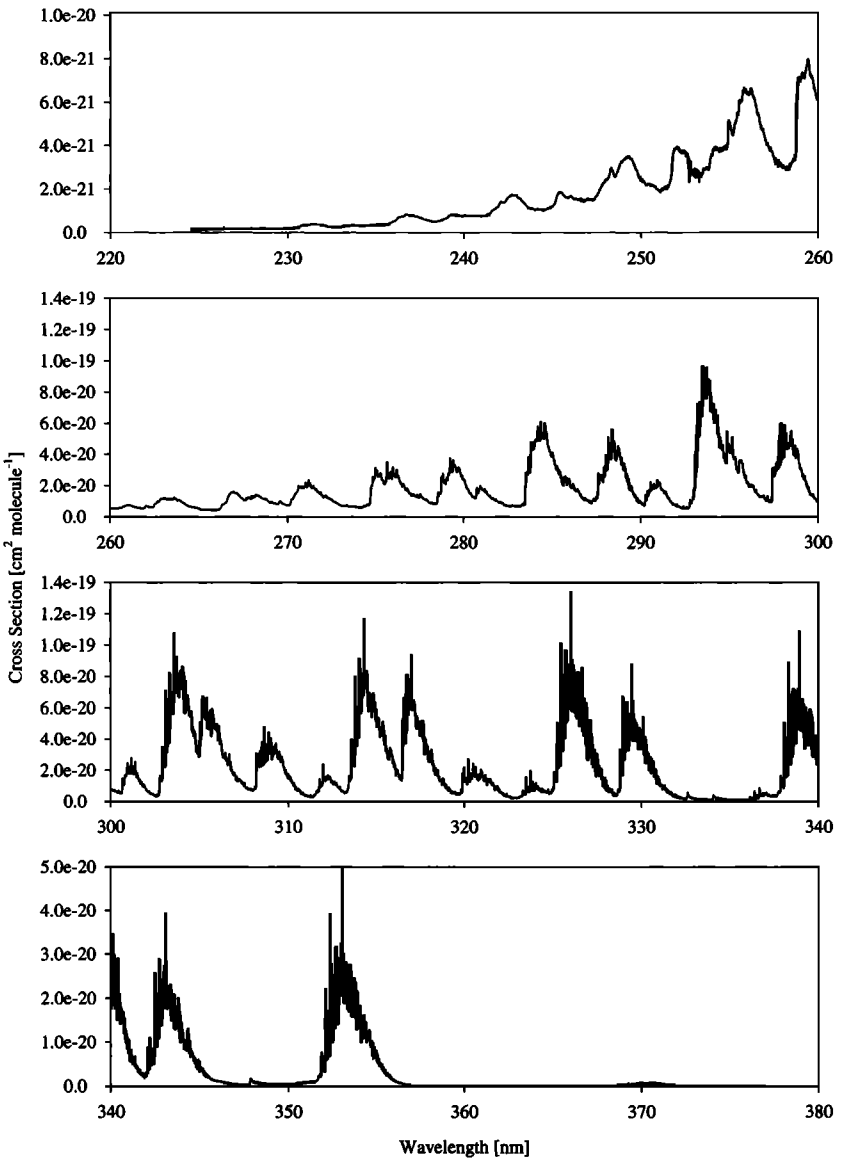

Figure 1. UV absorption spectrum of HCHO at 298 K in the range 225–375 nm obtained with the full resolution of ~0.04 nm.

[1966] and *Lide and Frederikse* [1997], respectively. The index n was calculated from

$$(n - 1) \times 10^8 = 8342.13 + 2406030[130 - (1000/\lambda_{vac})^2]^{-1} + 15997[38.9 - (1000/\lambda_{vac})^2]^{-1}, \quad (2)$$

where λ_{vac} is given in units of nanometers. Equation (2) is valid for dry "standard air" at 288 K and 101.325 kPa. Therefore the term $(n - 1)$ was corrected for the conditions (pressure p in pascals and temperature t in degrees Celsius) present in the experiments reported here through the multiplication by the correction factor c_n:

$$c_n = \frac{p[1 + p(61.3 - t) \times 10^{-10}]}{96095.4(1 + 0.003661t)} \quad (3)$$

3.2. Temperature Dependence of Absorption Cross Section

The HCHO absorption spectra were also measured at 223 K in the wavelength range 250–356 nm and at 253 and 323 K in the ranges from 312 to 326 and 335 to 349 nm. The spectra at the four temperatures 223, 253, 298 and 323 K are displayed in Figure 2 for the range from 336 to 346 nm. The measured high-resolution spectra were averaged over 0.1 nm intervals to eliminate most of the fine structure from the individual rotational bands for the sake of clarity in the plot. It can be seen in Figure 2 that temperature effects are the strongest at the maximum of the absorption bands, where lower temperatures result in larger absorptions. This temperature effect is reversed on the long wavelength side of the absorption bands; higher temperatures result in a higher absorption. At the steep, short wavelength side of the absorption band only a slight temperature effect is observed. Again, higher temperatures result here in a higher absorption. These observations are in agreement with the theory that UV absorption spectra alter with change in temperature because of the distribution of vibrational and rotational states.

A temperature gradient Γ was calculated for 0.1 nm intervals

Table 2. Absorption Cross Sections at 298 K σ(298 K) and Temperature Gradients of HCHO Γ Averaged Over 1 nm Intervals Centered at the Cited Wavelength λ

λ,* nm	σ(298 K), 10^{-21} cm^2 molecule^{-1}	Γ, 10^{-24} cm^2 molecule^{-1} K^{-1}	λ,* nm	σ(298 K), 10^{-21} cm^2 molecule^{-1}	Γ, 10^{-24} cm^2 molecule^{-1} K^{-1}	λ,* nm	σ(298 K), 10^{-21} cm^2 molecule^{-1}	Γ, 10^{-24} cm^2 molecule^{-1} K^{-1}
226	0.179		276	25.9	−2.040	326	68.7	−5.640
227	0.169		277	15.7	1.933	327	43.7	5.440
228	0.177		278	10.3	1.427	328	12.2	5.067
229	0.190		279	24.5	−2.547	329	31.2	−3.347
230	0.205		280	23.4	−0.680	330	38.6	−2.173
231	0.330		281	15.6	0.560	331	14.1	3.907
232	0.335		282	9.72	0.809	332	3.46	1.792
233	0.262		283	7.20	0.005	333	2.14	0.429
234	0.325		284	42.7	−8.720	334	1.59	−0.228
235	0.363		285	40.5	−1.800	335	0.966	−0.005
236	0.539		286	20.9	1.587	336	1.26	0.325
237	0.771		287	11.5	0.760	337	3.83	0.329
238	0.569		288	31.7	−4.707	338	19.2	1.600
239	0.682		289	32.2	−1.213	339	55.0	−6.587
240	0.782		290	11.7	1.707	340	31.5	5.520
241	0.775		291	18.4	−1.160	341	9.78	5.863
242	1.23		292	7.96	1.155	342	5.04	1.216
243	1.59		293	31.1	−4.907	343	19.2	−2.987
244	1.09		294	71.5	−10.213	344	12.7	0.187
245	1.31		295	40.6	3.827	345	4.36	2.765
246	1.63		296	24.8	2.120	346	1.19	0.541
247	1.51		297	13.6	1.387	347	0.441	−0.281
248	2.34		298	42.2	−4.933	348	0.757	−0.664
249	3.18		299	31.7	1.480	349	0.378	−0.560
250	2.57	0.203	300	9.63	4.267	350	0.360	−0.728
251	2.04	0.177	301	16.3	−2.573	351	0.894	−0.121
252	3.37	−0.072	302	8.52	−2.325	352	7.31	0.368
253	2.89	0.101	303	30.2	−3.600	353	22.8	−5.320
254	3.42	0.137	304	72.3	−4.827	354	16.5	0.600
255	4.50	0.272	305	47.4	4.173	355	6.96	2.456
256	6.29	0.169	306	42.9	0.320	356	1.48	−0.388
257	4.43	0.880	307	17.8	3.187	357	0.344	
258	3.07	0.681	308	13.8	0.333	358	0.186	
259	6.18	0.084	309	32.6	−3.867	359	0.111	
260	6.04	0.447	310	17.4	2.360	360	0.087	
261	6.60	0.093	311	4.61	0.075	361	0.100	
262	6.02	0.635	312	11.9	−1.227	362	0.211	
263	10.8	−0.813	313	9.02	−1.439	363	0.141	
264	9.47	0.580	314	56.5	0.720	364	0.094	
265	5.30	1.004	315	55.6	2.587	365	0.088	
266	5.38	0.431	316	25.4	4.760	366	0.085	
267	13.6	−0.880	317	57.9	−2.467	367	0.091	
268	12.4	−0.120	318	31.5	3.307	368	0.143	
269	9.90	1.116	319	9.75	2.532	369	0.297	
270	9.60	0.748	320	11.9	0.240	370	0.636	
271	19.4	−1.307	321	16.0	−2.187	371	0.572	
272	14.3	1.000	322	7.21	0.149	372	0.197	
273	8.10	1.228	323	3.27	0.389	373	0.113	
274	6.57	0.871	324	8.61	−0.456	374	0.091	
275	21.5	−2.733	325	15.4	2.213	375	0.087	

*Wavelengths are calibrated in air.

from the spectra measured at 223 and 298 K and is displayed in Figure 3 together with the spectrum at 223 K. To calculate the UV absorption spectrum at a certain temperature T, the following equation is used:

$$\sigma(\lambda, T) = \sigma(\lambda, 298\ \text{K}) + \Gamma(T - 298\ \text{K}) \quad (4)$$

Equation (4) is an easy mathematical expression for describing the temperature dependence with sufficient accuracy for all atmospheric applications, but it does not represent the theoretically expected relation. In Table 2, absorption cross sections at 298 K and temperature gradients, both averaged over 1 nm intervals, are listed for the wavelength ranges 226–375 and 250–356 nm, respectively. Cross sections at 298 and 223 K and the temperature gradient Γ averaged over intervals commonly used in atmospheric modeling are listed in Table 3 and are available in different resolutions in digital form from the authors (see section 4). Error limits of the temperature gradient are ±7% calculated from the error propagation. Spectra calculated according to (2) at T = 248 K and T = 332 K were compared with the measured spectra at these temperatures. Maximum deviations from the observed to the calculated spectra of 7% were observed, mainly in the regions with the strongest absorption.

The resolution or the intervals over which high-resolution

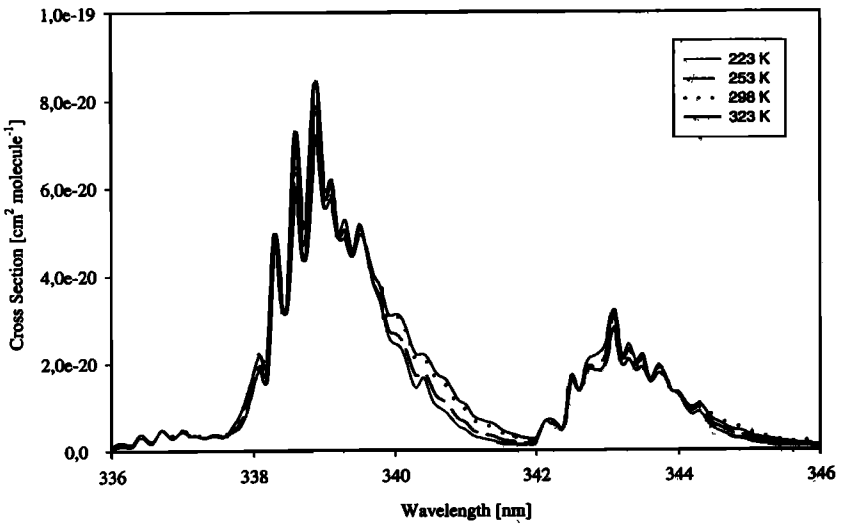

Figure 2. Absorption spectra of HCHO at 298, 273, 248, and 223 K in the range 336–346 nm with the reduced resolution of 0.1 nm.

HCHO absorption spectra are averaged have a large effect on the temperature gradient. In Figure 4 the temperature gradient as a function of wavelength is presented for spectra averaged over 0.01, 0.1, and 1.0 nm and "atmospheric intervals." As the size of the intervals increases, the temperature effect on the absorption cross section decreases. For the smallest intervals the temperature effect for individual rotational bands can be detected, and with 1.0 nm intervals the temperature gradient for vibrational bands is still sufficiently represented. As can be seen in Figure 4, for intervals larger than 1.0 nm the representation of the temperature gradient is inadequate, for example, for the intervals commonly used in atmospheric modeling. If temperature-dependent absorption cross sections of HCHO are used for model calculation, care must be taken that intervals are used that guarantee a correct representation.

3.3. Comparison of the Low-Resolution Room Temperature Spectrum With Previous Measurements

Comparisons were made with previous measurements of the absorption cross sections of formaldehyde. In Table 1 these earlier measurements are listed together with the most important experimental information. For this comparison, data from this work were integrated over intervals commonly used for atmospheric modeling to match the intervals given in the other works. It is important to notice that the work done by *Cantrell et al.* [1990] and by *Rogers* [1990] report vacuum wavelengths, which typically yields a wavelength shift of ~0.1 nm in the range investigated. Accordingly, corrections were made to be able to compare the spectra at the conditions used in this study. Spectra from *Bass et al.* [1980], *Moortgat et al.* [1980], *Cantrell*

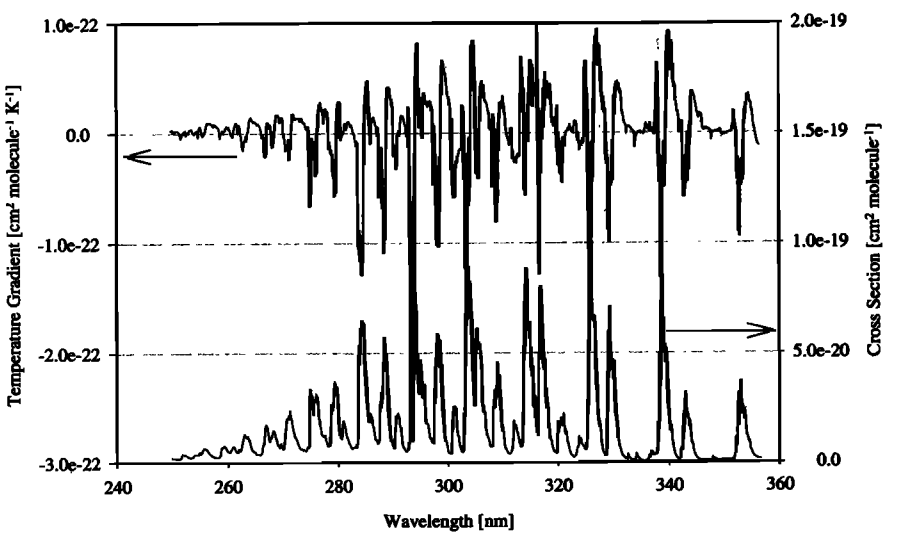

Figure 3. Temperature gradient of HCHO (0.1 nm intervals) in the range 250–356 nm. The HCHO absorption spectrum at 223 K is included for comparison.

Table 3. Absorption Cross Sections at 298 and 223 K and Temperature Gradients of HCHO Averaged Over Intervals Used in Atmospheric Modeling

Wavelength,* nm	Wavelength Range,* [nm]	$\lambda(298)$, $\times 10^{-20}$ cm^2 molecule^{-1}	$\lambda(223)$, $\times 10^{-20}$ cm^2 molecule^{-1}	Γ, $\times 10^{-24}$ cm^2 molecule^{-1} K^{-1}
226.0	224.7–227.3	0.0166		
228.6	227.3–229.9	0.0181		
231.2	229.9–232.6	0.0303		
233.9	232.6–235.3	0.0313		
236.7	235.3–238.1	0.0625		
239.5	238.1–241.0	0.0704		
242.4	241.0–243.9	0.126		
245.4	243.9–246.9	0.139		
248.5	246.9–250.0	0.254		
251.6	250.0–253.3	0.270	0.265	0.720
254.8	253.2–256.4	0.449	0.435	1.77
258.1	256.4–259.7	0.478	0.438	5.35
261.4	259.7–263.2	0.698	0.687	1.45
264.9	263.2–266.7	0.736	0.698	5.00
268.5	266.7–270.3	1.13	1.11	2.80
272.1	270.3–274.0	1.30	1.27	3.87
275.9	274.0–277.8	1.84	1.89	−5.73
279.7	277.8–281.7	1.86	1.89	−3.60
283.7	281.7–285.7	2.55	2.72	−22.3
287.8	285.7–289.9	2.33	2.38	−7.47
292.0	289.9–294.1	2.66	2.93	−34.9
296.3	294.1–298.5	3.28	3.23	5.73
300.8	298.5–303.0	1.60	1.58	2.80
305.4	303.0–307.7	4.42	4.43	−1.73
310.1	307.7–312.5	1.63	1.67	−5.47
315	312.5–317.5	4.09	4.03	8.40
320	317.5–322.5	1.53	1.47	8.13
325	322.5–327.5	2.79	2.76	3.87
330	327.5–332.5	1.99	1.91	10.5
335	332.5–337.5	0.196	0.183	1.71
340	337.5–342.5	2.39	2.28	15.2
345	342.5–347.5	0.758	0.755	0.480
350	347.5–352.5	0.194	0.220	−3.40
355	352.5–357.5	0.961		
360	357.5–362.5	0.0139		
365	362.5–367.5	0.0010		
370	367.5–372.5	0.0369		

*Wavelengths are calibrated in air.

et al. [1990], *Rogers* [1990], and this study were available in digital form and in high resolution. The cross sections from *McQuigg and Calvert* [1969] were taken from the table in the literature [*Calvert et al.*, 1972] where values averaged over 10 nm intervals were reported. In Figure 5a the HCHO absorption cross sections measured in this study are compared with previous studies, and in Figure 5b the cross sections relative to this work are displayed.

The cross sections obtained in this study are the second highest of all measurements. Only *McQuigg and Calvert* [1969] reported larger values. Their work covered the wavelength range from 285 to 365 nm, and integrated absorptions over 10 nm intervals were reported. Over the range 285–365 nm, absorption cross sections are ~17% larger than those observed in this study for the same spectral region. Deviations are between +3 and +18% for wavelengths shorter than 330 nm but increase dramatically for longer wavelengths where absorption cross sections decrease. *Bass et al.* [1980] measured in the range 260–358 nm and reported their results in intervals used for atmospheric modeling and 10 nm intervals. Their values are on average 21% lower than the absorption cross sections measured in this study. For wavelengths below 310 nm the values of *Bass et al.* [1980] are ~10–15% lower, but for longer wavelengths it is apparent that in regions with stronger absorptions much larger deviations are found, as high as 50% of the value measured here. However, the weaker absorptions in the region 310–360 nm are still in the range of 10–20% too low. *Cantrell et al.* [1990] attributed these discrepancies in regions near the peaks of strong absorbing bands to the failure of *Bass et al.* [1980] to account for nonlinearity of formaldehyde in the Beer-Lambert behavior as a function of column amount. However, these strong deviations are not observed for the strong absorption bands at wavelengths shorter that 310 nm and, in particular, not for the strongest absorption band at around 303 nm. There is a very good agreement between the *Moortgat et al.* [1980] measurements and this work. The overall band intensity matches within the error limits (±5%). Larger relative deviations are only observed where the noise of the measurements becomes a problem at wavelengths shorter than 240 and larger than 357 nm. *Cantrell et al.* [1990] measured their HCHO spectrum only at wavelengths larger 300 nm. For this range the overall absorption is 10% lower than the cross sections determined in this work. Deviations of more the 20% for individual 2.5 nm intervals are only observed where the absorption cross sections drop down to values smaller than 1.0×10^{-20} cm^2 molecule^{-1}. A comparison of the room temperature study of *Rogers* [1990] is possible for almost the entire wavelength range from 240 to 360 nm. In this range his reported average absorp-

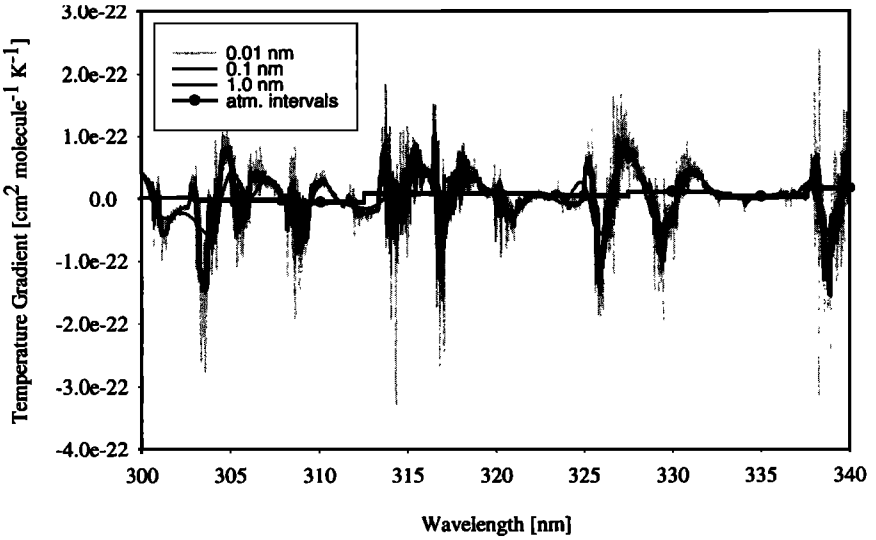

Figure 4. Temperature gradients of HCHO in the range 300–340 nm averaged over 0.01, 0.1, and 1.0 nm and atmospheric intervals.

tion cross section is 11% smaller than the value reported in this work. In the region with the strongest absorptions, between 280 and 320 nm, both data sets are in good agreement (within 5%), but deviations increase as absorptions decrease. The integrated absorption between 240 and 260 nm, the value reported by *Rogers* [1990], is <50% of that observed in this study.

In a second part of this comparison the spectrum of formaldehyde was divided into four parts (230–250, 250–290, 290–355, and 355–370 nm), which were then individually analyzed. Again, we used the data sets averaged over intervals commonly used for atmospheric modeling in order to eliminate any effects of the different resolution and temperature and the 10 nm averaged spectrum reported by *McQuigg and Calvert* [1969].

1. In this work, absorptions cross sections in the range 230–250 nm are presented for the first time with reasonable signal to noise levels. Measurements of *Moortgat et al.* [1980] and *Rogers* [1990], which also cover at least partially this range, are much too noisy to deduce reliable values from them. The

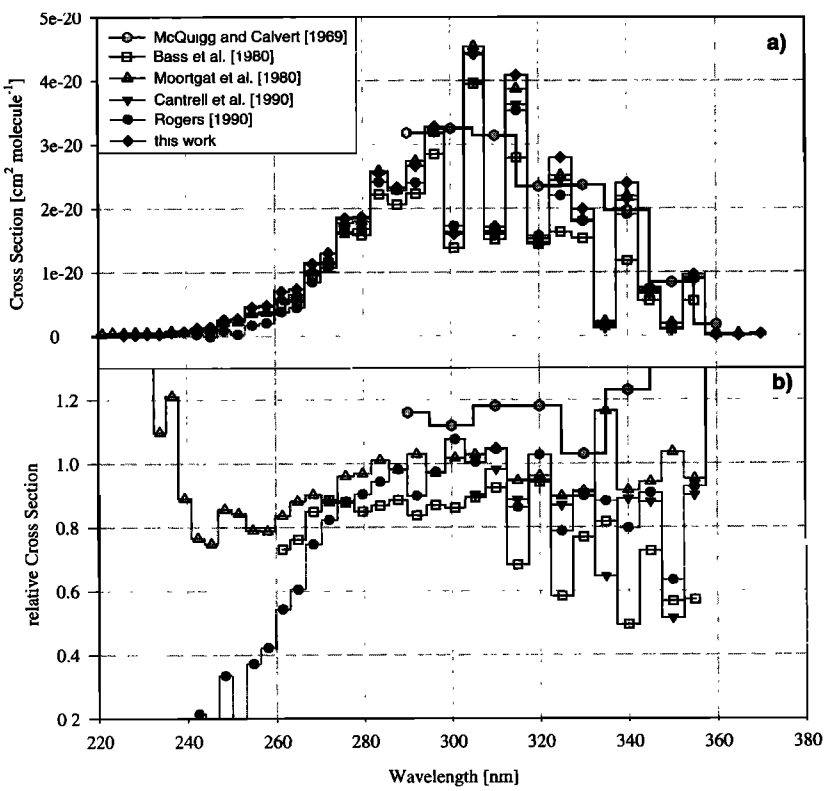

Figure 5. (a) Comparison of integrated (2.5 nm) intervals of the HCHO absorption cross section with earlier studies. (b) Relative cross section of earlier studies.

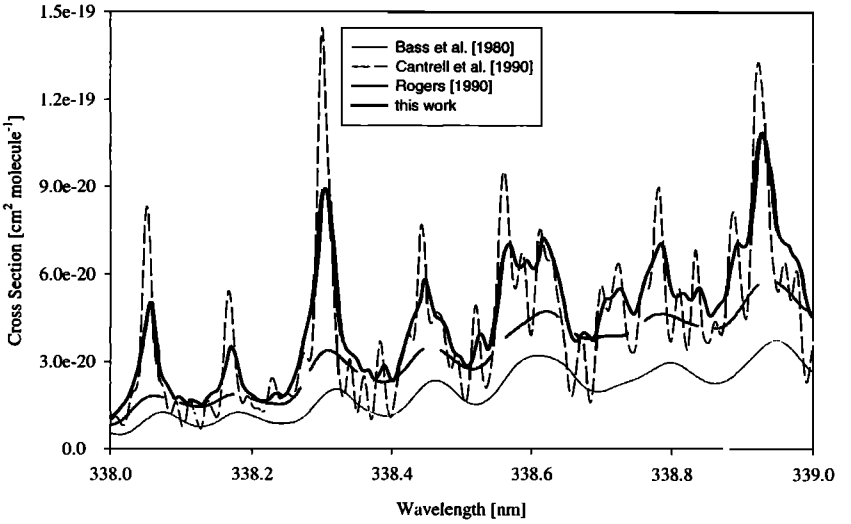

Figure 6. Comparison of the high-resolution spectrum with earlier studies in the range 338–339 nm. For the resolution of the individual studies, see Table 1.

advantage of measuring small individual optical windows instead of the entire spectrum becomes apparent. Using this technique, it is possible to adjust the optical thickness of the sample for each segment in such a way that tolerable signal to noise levels are achieved.

2. Measurements of *Bass et al.* [1980], *Moortgat et al.* [1980], *Rogers* [1990], and this work are available for the range 250–290 nm. There is a general agreement between all these measurements for wavelengths longer 280 nm where deviations are smaller than 10%. However, for decreasing wavelengths the absorption cross sections from these measurements show increasing deviations. One reason might be the increasing noise levels in the older measurements. That is the most evident for the spectrum from *Rogers* [1990]; the absorption cross sections from *Bass et al.* [1980] and *Moortgat et al.* [1980] only decrease to ~80% of the cross sections observed in this work.

3. The range 290–355 nm is the most important for atmospheric photolysis of formaldehyde. In that range the results of all measurements agree quite well except those of *McQuigg and Calvert* [1969] and *Bass et al.* [1980]. The integrated band strength for that range from the four groups agrees to within 5% of their average. *Cantrell et al.* [1990] and *Rogers* [1990] report the lowest values, whereas the highest values are from this work. The dominant contribution to the overall band intensity originates from the strong absorbing peaks. For strong absorptions where a nonlinearity Beer-Lambert behavior is expected it is essential to measure at very low optical thickness. In this work we measured at 500 ± 50 mtorr HCHO partial pressure, the lowest of all the studies, which corresponds to a maximum optical density of 0.1. The largest uncertainties exist for the regions with the lowest absorptions. That is expected since it is almost impossible to measure in a single scan with same relative accuracy absorbances that are 2 orders of magnitude apart. However, one should notice that these relative uncertainties are not so crucial for atmospheric modeling.

4. For wavelengths larger than 355 nm, where absorption cross sections are $<1 \times 10^{-21}$ cm^2 molecule^{-1}, the same can be said as for the region below 240 nm. *Moortgat et al.* [1980] and *Rogers* [1990] also report values for that range, but their measured spectra are very noisy.

3.4. Comparison of the High-Resolution Spectrum With Previous Measurements

In Figure 6 the cross sections of HCHO from 339 to 340 nm as measured in high-resolution by *Bass et al.* [1980], *Cantrell et al.* [1990], *Rogers* [1990] and this work are compared. The two data sets of *Bass et al.* [1980] and *Rogers* [1990] with the apparent lower resolution are too coarse to reveal the individual rotational bands. The spectrum of *Rogers* [1990] (a spectrum in a resolution of ~0.04 nm was supplied by Rogers) describes the weaker absorptions between the peaks quite well but fails to describe the strong absorption bands that resulted in the lower cross section for the entire band (see Figure 5). The shape of the spectra from these two studies is identical, but as noticed above, the reported cross sections from *Bass et al.* [1980] are too low for that vibrational band. The spectrum from *Cantrell et al.* [1990] exhibits the best resolution of the spectra shown here. The rotational bands have the smallest half widths of full maximum, and therefore the peak cross sections are the largest, and the minima between the peaks are the lowest. Overall, their cross sections are ~10% lower than those observed here.

3.5. Comparison of the Temperature Gradient With Previous Measurements

In some of the earlier studies the temperature dependence of the UV absorption spectrum has been investigated, but there are just the measurements from *Bass et al.* [1980] and *Cantrell et al.* [1990] where actual data are reported. *McQuigg and Calvert* [1969] and *Rogers* [1990] did not measure their HCHO absorption spectra as a function of temperature. *Moortgat et al.* [1980] measured at different temperatures but used a very low resolution of 0.5 nm that is too coarse to reveal the distribution of rotational lines contained within an absorption band.

For this comparison we calculated the temperature gradient Γ as described in (4) for the studies of *Bass et al.* [1980] and *Cantrell et al.* [1990] in 0.1 nm. In Figure 7 the temperature gradient Γ is displayed as a function of the wavelength for the three studies. There is a remarkable agreement between this study and the early study from *Bass et al.* [1980] for wave-

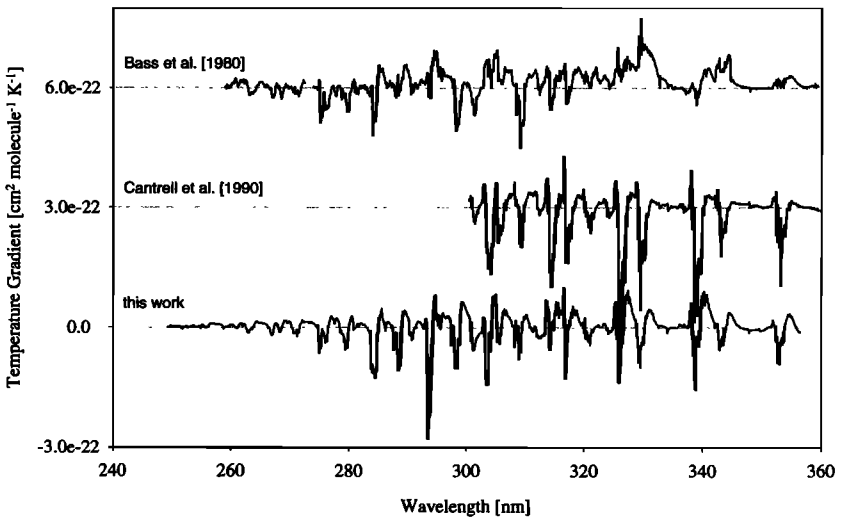

Figure 7. Comparison of the temperature gradient Γ (0.1 nm intervals) as a function of the wavelength from this study, *Bass et al.* [1980] (offset 6×10^{-22} cm^2 molecule^{-1}) and *Cantrell et al.* [1990] (offset 3×10^{-22} cm^2 molecule^{-1}) in the range 250–360 nm.

lengths shorter than 304 nm, except for two strong absorption bands at 288 and 294 nm. In both studies the same dependence at the maximum and at the tails of the absorption bands is observed. This agreement does not continue for wavelengths larger than 304 nm. At these wavelengths the temperature gradient measured by *Bass et al.* [1980] shows some unexpected behavior at the maxima of absorption bands, where a decrease in the cross section with decreasing temperatures is observed. This is particularly apparent for the bands near 304, 306, 326, 330, 343, and 353 nm, where actually, the opposite of the expected behavior is seen. As mentioned above, *Bass et al.* [1980] failed to account for nonlinearity in the Beer-Lambert behavior for HCHO at the strong absorbing bands in this region. Therefore it seems very likely that this might have caused these unexpected results.

The results for the temperature dependence from this study and those from *Cantrell et al.* [1990] reveal the same anticipated behavior. The differences between both studies lay in the absolute magnitude of the temperature gradient at the maximum and at the long wavelength flank of the absorption bands. For wavelengths between 300 and 320 nm the differences are only minor but are very obvious for wavelengths larger than 320 nm. In Figure 8 the temperature gradients from both studies are displayed in the range 322–332 nm. Figure 8 shows that regions with small absorbances (322–225) and at the short wavelength flank (225–226 and 328–329 nm) in both studies agree very well. At the maxima, near 226 nm, *Cantrell et al.* [1990] measured a temperature gradient that is about twice as large as that observed in this study. On the long wavelength flank (326–328 and 329–332 nm) this negative temperature dependence persists toward longer wavelengths (within one absorption band) in the study of *Cantrell et al.* [1990]. As a result of this pronounced negative temperature effect, the spectra calculated from the data reported by *Cantrell et al.* [1990] at lower temperatures (e.g., 223 K) have a larger integrated (300–360 nm) absorption than the spectrum at room

Figure 8. Temperature gradient Γ (0.1 nm intervals) as a function of the wavelength from this study and from *Cantrell et al.* [1990] in the range 322–332 nm.

temperature. For the range 303.3–256.6 nm the average cross section at 298 K is 1.71×10^{-20} cm^2 molecule^{-1}, and at 223 K, it is 1.81×10^{-20} cm^2 molecule^{-1}. The results from this study show that there is no change of the average cross section with changing temperatures. The increase of the absorption near the maximum of the peak is completely compensated with the decrease in the flanks of the band. In this study average cross sections of 1.89×10^{-20} and 1.87×10^{-20} cm^2 molecule^{-1} were calculated for 298 and 223 K, respectively.

4. Conclusion

In this study, HCHO UV absorption cross sections and temperature gradients are presented for the wavelength range 225–375 nm. Results from this investigation provide for the first time a complete data set over the entire absorption band in high resolution and with minimized systematic errors because of the low HCHO concentrations used and the employed sample preparation. The measured cross sections are ~5–10% larger than the previously recommended cross sections. The temperature gradient obtained in this work covers the range 250–356 nm and exhibits the same general shape as the temperature gradients of previously recommended spectra but differs in the shape of the individual rotational bands. In model calculations the intervals over which the HCHO spectrum is averaged should not exceed 1.0 nm to assure a correct representation of the cross sections and the temperature gradient.

The data from this study are available in digital form from the authors (G. K. M.; moo@mpch-mainz.mpg.de). These data sets contain the absorption cross sections measured in this work at 298 K for the wavelength range 225–375 nm (wavelength calibration in air at ~750 torr) and the absorption cross sections at 223 K and the temperature gradient for the wavelength range 250–356 nm. Spectra and temperature gradients are reported in intervals averaged over 0.01, 0.1, and 1.0 nm and in intervals commonly used for atmospheric modeling.

References

Altshuller, A. P., Production of aldehydes as primary emissions and from secondary atmospheric reactions of alkenes and alkanes during the night and early morning hours, *Atmos. Environ., Part A, 27*, 21–31, 1993.

Anderson, L. G., J. A. Lanning, R. Barrell, J. Miyagishima, R. H. Jones, and P. Wolfe, Sources and sinks of formaldehyde and acetaldehyde: An analysis of Denver's ambient concentration data, *Atmos. Environ., 30*, 2113–2123, 1996.

Atkinson, R., E. C. Tuazon, and S. M. Aschmann, Products of the gas-phase reactions of O_3 with alkenes, *Environ. Sci. Technol., 29*, 1860–1866, 1995.

Atkinson, R., D. L. Baulch, R. A. Cox, R. F. Hampson Jr., J. A. Kerr, M. J. Rossi, and J. Troe, Evaluated kinetics, photochemical and heterogeneous data for atmospheric chemistry: Supplement V, *J. Phys. Chem. Ref. Data, 26*, 521–1011, 1997.

Bass, A. M., L. C. Glasgow, C. Miller, J. P. Jesson, and D. L. Filkin, Temperature dependent absorption cross section for formaldehyde (CH_2O): The effect of formaldehyde on stratospheric chlorine chemistry, *Planet. Space Sci., 28*, 675–679, 1980.

Benning, L., and A. Wahner, Measurements of atmospheric formaldehyde (HCHO) and acetaldehyde (CH_3CHO) during POPCORN 1994 using 2.4-DNPH coated silica cartridges, *J. Atmos. Chem., 31*, 105–117, 1998.

Calvert, J. G., J. A. Kerr, K. L. Demerjian, and R. D. McQuigg, Photolysis of formaldehyde as a hydrogen atom source in the lower stratosphere, *Science, 175*, 751–752, 1972.

Cantrell, C. A., J. A. Davidson, A. H. McDaniel, R. E. Shetter, and J. G. Calvert, Temperature-dependent formaldehyde cross sections in the near ultraviolet spectra region, *J. Phys. Chem., 94*, 3902–3908, 1990.

Carlier, P., H. Hannachi, and G. Mouvier, The chemistry of carbonyl compounds in the atmosphere: A review, *Atmos. Environ., 20*, 2079–2099, 1986.

Crosswhite, D. H. M., The iron-neon-hollow-cathode spectrum, *J. Res., 79*, 5–48, 1975.

DeMore, W. B., S. P. Sander, D. M. Golden, R. F. Hampson, M. J. Kurylo, C. J. Howard, A. R. Ravishankara, C. E. Kolb, and M. J. Molina, Chemical kinetics and photochemical data for use in stratospheric modeling, *JPL Publ. 97-4*, Jet Propul. Lab., Pasadena, Calif., 1997.

Dieke, G. H., and G. B. Kristiakowsky, The structure of the ultraviolet absorption spectrum of formaldehyde, *Phys. Rev., 45*, 4–28, 1934.

Edlen, B., The refraction index of air, *Metrologia, 2*, 71–80, 1966.

Fried, A., S. Sewell, B. Henry, B. P. Wert, T. Gilpin, and J. Drummond, Tunable diode laser absorption spectrometer for ground-based measurements of formaldehyde, *J. Geophys. Res., 102*, 6253–6266, 1997.

Grosjean, D., Ambient levels of formaldehyde, acetaldehyde, and formic acid in southern California: Results of a one-year base-line study, *Environ. Sci. Technol., 25*, 710–715, 1991.

Grosjean, E., E. L. Williams II, and D. Grosjean, Ambient levels of formaldehyde and acetaldehyde in Atlanta, Georgia, *J. Air Waste Manage. Assoc., 43*, 469–674, 1993.

Grosjean, E., J. B. De Andrade, and D. Grosjean, Carbonyl products of the gas-phase reaction of ozone with simple alkenes, *Environ. Sci. Technol., 30*, 975–983, 1996.

Harder, J. W., A. Fried, S. Sewell, and B. Henry, Comparison of tunable diode laser and long-path ultraviolet/visible spectroscopy measurements of ambient formaldehyde concentrations during the 1993 OH photochemistry experiment, *J. Geophys. Res., 102*, 6267–6282, 1997.

Heikes, B., et al., Formaldehyde methods comparison in the remoter lower troposphere during the Mauna Loa Photochemistry Experiment 2, *J. Geophys. Res., 101*, 14,741–14,755, 1996.

Henri, V., and S. A. Schou, Struktur und Aktivierung der Molekel des Formaldehyds: Eine Analyse auf Grund des ultravioletten Absorptionsspektrums des Dampfes, *Z. Phys., 49*, 774–826, 1928.

Jacob, D. J., et al., Origin of ozone and NO_x in the tropical troposphere: A photochemical analysis of aircraft observations over the South Atlantic Basin, *J. Geophys. Res., 101*, 24,235–24,250, 1996.

Jaegle, L., D. J. Jacob, W. H. Brune, D. Tan, I. C. Faloona, A. J. Weinheimer, B. A. Ridley, T. L. Campos, and G. W. Sachse, Sources of HO_x and production of ozone in the upper troposphere over the United States, *Geophys. Res. Lett., 25*, 1709–1712, 1998.

Lee, Y.-N., X. Zhou, and K. Hallock, Atmospheric carbonyl compounds at a rural southeastern United States site, *J. Geophys. Res., 100*, 25,933–25,944, 1995.

Lee, Y.-N., et al., Atmospheric chemistry and distribution of formaldehyde and several multioxygenated carbonyl compounds during the 1995 Nashville/Middle Tennessee Ozone Study, *J. Geophys. Res., 103*, 22,449–22,462, 1998.

Levi, H., Normal atmosphere: Large radical and formaldehyde concentrations predicted, *Science, 173*, 141–143, 1971.

Lide, D. R., and H. P. R. Frederikse (Eds.), *CRC Handbook of Chemistry and Physics*, 78th ed., CRC Press, Boca Raton, Fla., 1997.

Lipari, F., J. M. Dasch, and W. F. Scuggs, Aldehyde emissions from wood-burning fireplaces, *Environ. Sci. Technol., 18*, 326–330, 1984.

Lowe, D. C., and U. Schmidt, Formaldehyde (HCHO) measurements in the nonurban atmosphere, *J. Geophys. Res., 88*, 10,844–10,858, 1983.

Massachusetts Institute of Technology (MIT), *Massachusetts Institute of Technology Wavelength Tables*, MIT Press, Cambridge, Mass., 1969.

McQuigg, R. D., and J. G. Calvert, The photolysis of CH_2O, CD_2O, CHDO, and CH_2O-CD_2O mixtures at xenon flash lamp intensities, *J. Am. Chem. Soc., 91*, 1590–1604, 1969.

Meller, R., and G. K. Moortgat, $CF_3C(O)Cl$: Temperature-dependent (223-298 K) absorption cross-sections and quantum yields at 254 nm, *J. Photochem. Photobiol. A, 108*, 105–116, 1997.

Meller, R., W. Raber, J. N. Crowley, M. E. Jenkins, and G. K. Moortgat, The UV/visible absorption spectrum of methylglyoxal, *J. Photochem. Photobiol. A, 62*, 163–171, 1991.

Moortgat, G. K., W. Kippel, K. H. Möbus, W. Seiler, and P. Warneck, Laboratory measurements of photolytic parameters for formaldehyde, *FAA Rep. N. FAA-EE-80-47*, Fed. Aviation Admin., Washington, D.C., 1980.

Moortgat, G. K., W. Seiler, and P. Warneck, Photodissociation of HCHO in Air: CO and H_2 quantum yields at 220 K and 300 K, *J. Chem. Phys.*, *78*, 1185–1190, 1983.

Rogers, J. D., Ultraviolet absorption cross sections and atmospheric photodissociation rate constants of formaldehyde, *J. Phys. Chem.*, *94*, 4011–4015, 1990.

Singh, H. B., M. Kanakidou, P. J. Crutzen, and D. J. Jacob, High concentrations and photochemical fate of oxygenated hydrocarbons in the global troposphere, *Nature*, *378*, 50–54, 1995.

Spence, R. B., and A. Wilde, the preparation of liquid monomeric formaldehyde, *J. Chem. Soc.*, 338–340, 1935.

Thomas, W., E. Hegels, S. Slijkhuis, R. Spurr, and K. Chance, Detection of biomass burning combustion products in southeast Asia from backscatter data taken by the GOME spectrometer, *Geophys. Res. Lett.*, *25*, 1317–1320, 1998.

R. Meller and G. K. Moortgat, Atmospheric Chemistry Department, Max-Planck-Institut für Chemie, Postfach 3060, 55020 Mainz, Germany. (moo@mpch-mainz.mpg.de)

(Received August 3, 1999; revised October 11, 1999;
accepted October 18, 1999.)